

COMMUNICATION

Binary encoding of peptide sequences into differential antimicrobial mechanisms

Zvi Hayouka,^{* [a]} Angelo Bella,^[b] Tal Stern,^[a] Santanu Ray,^[c] Haibo Jiang,^[d] Chris R. M. Grovenor^[e] and Maxim G. Ryadnov^{*[b]}

Abstract: binary encoding of peptide sequences into differential antimicrobial mechanisms is reported. Such sequences are random in composition, but controllable in chain length, are assembled from the same two amino acids, but differ in the stereochemistry of one. Regardless of chirality the sequences lyse bacteria including "superbugs" MRSA and VRE. Sequences with persistent chirality – homochiral sequences – assemble into antimicrobial pores and form contiguous helices that are biologically promiscuous and hemolytic. By contrast, heterochiral sequences that lack such persistence selectively attack bacterial membranes without oligomerising into visible pores. The results offer a mechanistic rationale for designing membrane-selective and sequence-independent antimicrobials.

An effective solution to these issues may be found in peptide diastereomers^[15] that are commonly used to explore the dependence of biological activities on α -helix formation.^[16] Current evidence suggests that single L-to-D mutations in all-L sequences lead to decreased helicity and decreased hemolytic activities without affecting antimicrobial properties.^[15,16] This empirical relationship renders helix formation unnecessary for antimicrobial activity.^[17] However, a direct observation of how diastereomeric helices exhibit differential cytolytic responses with respect to specific membrane-mediated mechanisms is as crucial as it is lacking.

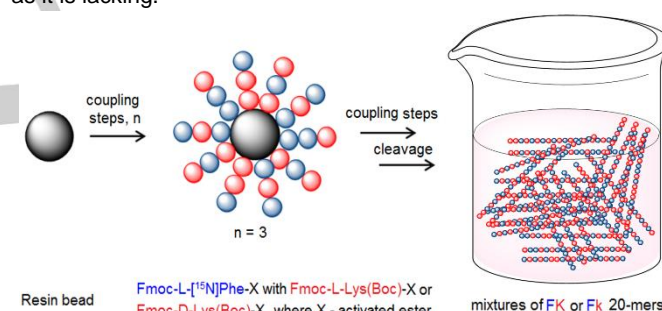


Figure 1. Synthesis of sequence-random peptide mixtures. A schematic representation of the solid-phase synthesis of FK and Fk mixtures using equimolar mixtures of pre-activated Fmoc-L-[¹⁵N]Phe-X with Fmoc-L-Lysine(Boc)-X or with Fmoc-D-Lysine(Boc)-X. 20 coupling steps followed by cleavage from the resin generate the 2²⁰ libraries of random FK and Fk 20-mers. ¹⁵N-labelling was used to enable the chemical imaging of peptides in membranes.

Antimicrobial peptides (AMPs) hold promise as anti-infective agents in the post-antibiotic era.^[1] A widespread resistance against these molecules, which attack both growing and dormant microbial cells, is unknown.^[2] Antimicrobial mechanisms typically involve poration and intracellular targeting,^[3] are often multi-target and therefore endow AMPs with a substantial clinical potential.^[4] A counterargument against their use in clinic is two-fold. Firstly, antimicrobial resistance is relentless.^[5] Resistance mechanisms need not require microbial membranes to re-build as it is usually assumed,^[1-4] and can ensue via co-folding antagonists^[6] or cell-surface alterations reducing the negative charge of membranes.^[7] Secondly, despite their apparent diversity AMPs share similar structural attributes, while adopting membrane-disrupting amphipathic conformations.^[8,9] In this light, the origin of an AMP to be developed as a drug is not as important as its prolonged exposure to that part of our immune system that relies on own AMPs. At least partly, the first point is addressed by the tendency of antimicrobial sequences to incorporate motifs that compromise co-folding with antagonists.^[10] Mimicking AMPs by unnatural oligomers,^[11] can provide artificial analogues exhibiting similar activities with a higher enzymatic stability and disfavoured oligomerisation capacities.^[12] None of these, however, addresses the second point as peptide conformations can be cytolytic.^[13,14]

Herein, we reason that folding propensity can be diastereomerically randomised to ensure peptide selectivity towards microbial membranes without affecting erythrocyte membranes. Random homochiral sequences of hydrophobic and cationic amino acids are likely to be cytolytic due to the uncontrollably high ratios of hydrophobic-to-polar residues in individual sequences.^[18] Chirality, and hence folding, in these sequences is persistent, thus increasing the probability of hemolytic effects.^[13,14] Sequences assembled from randomly distributed L- and D-amino acids lack such persistence. We further reason that homochiral helices must be able to assemble in anionic phospholipid bilayers in a manner similar to that of sequence-defined AMPs. This is in contrast to heterochiral peptides that cannot assemble cooperatively and whose membrane insertion is limited to random oligomerisation. With this in mind, we generated two libraries of randomised 20-mer sequences. Each was assembled from two amino acids – hydrophobic phenylalanine and cationic lysine. In one library, both amino acids are in L configuration, in the other all lysines are in D configuration. The libraries, termed FK and Fk, where k denotes D-lysine (Fig 1), were prepared by standard Fmoc-solid phase synthesis protocols, with the two amino acids used as an equimolar mixture in each coupling step. The differences in

[a] Dr Z. Hayouka, Ms Tal Stern
Institute of Biochemistry, Food Science and Nutrition,
The Hebrew University of Jerusalem, Rehovot, 76100, Israel
E-mail: zvi.hayouka@mail.huji.ac.il

[b] Dr M. G. Ryadnov, Dr A. Bella
National Physical Laboratory
Teddington, TW11 0LW (UK)
E-mail: max.ryadnov@npl.co.uk

[c] Dr S. Ray
SET, University of Brighton, BN2 4GJ (UK)

[d] Dr J. Haibo
CMCA, University of Western Australia,
Perth, 6009, Australia

[e] Prof. C. R. M. Grovenor
Department of Materials, University of Oxford,
Oxford OX1 3PH, UK

Supporting information is given via a link at the end of the document.

reactivity of the two amino acids in activated forms were deemed marginal for resulting mixtures to deviate from the starting equimolar combination. Indeed, the amino-acid analysis of the resulting mixtures confirmed that the ratio was maintained (Fig S1 in Supplementary information).^[18] Moreover, the returned ratios were nearly identical for the two mixtures, indicating that growing peptide chains did not favor or discriminate the incorporation of amino acids based on chirality (Fig S1).^[19]

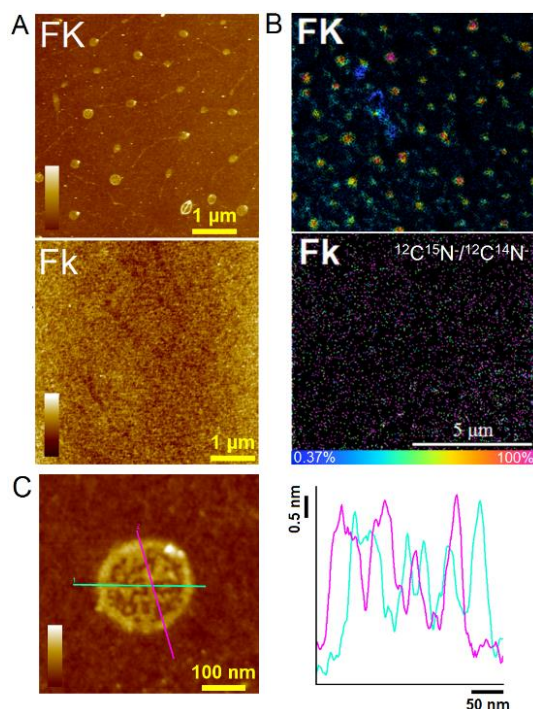


Figure 2. Enantiomerically defined poration in supported lipid bilayers. Topographic (A) and chemical (B) images of SLBs treated with the homochiral (FK) and heterochiral (Fk) mixtures ¹⁵N-labelled at phenylalanyl residues. Color (height) scales: 5 nm for FK and 1.5 nm for Fk. Note the smaller scale for Fk. (B) SIMS images of ¹²C¹⁵N/¹²C¹⁴N⁺ signal ratio are expressed as hue saturation images, which are the sums of sequential images used to enhance the statistical significance of the measured ratios. The rainbow scale changes from blue (natural abundance of 0.37%) to pink (100%). (C) A high-resolution topographic AFM image of an individual pore (upper) with cross-sections along the highlighted lines (lower). Color (height) scale is 5.5 nm. Incubation conditions: 10 μM peptide (total), 10 L/P (lipid-peptide) molar ratio, pH 7, 20 °C.

Consistent with this, Circular Dichroism (CD) spectra for both mixtures revealed a dominating minimum at ~230 nm and additional negative and positive bands at ~215 nm and ~220 nm.^[20,21] Attributable to aromatic π - π^* transitions, these indicate superimposed aromatic bands of a constrained chiral environment suggesting folding (Fig S2).^[20-22] Furthermore, the spectra were characteristic of helix-rich lysyl-phenylalanyl oligomers^[23] and were reminiscent of distorted and attenuated signals typical of helical assemblies.^[24] Thus, the spectra are supportive of pre-folding in solution for both mixtures that is likely to be accompanied by oligomerisation.

To further understand this non-responsive mode of folding, CD spectra were obtained for the mixtures in reconstituted membranes.^[25] Anionic and zwitterionic unilamellar vesicles, AUVs and ZUVs, respectively, provided microbial and mammalian membrane mimetics,^[25,26] while weakly anionic AUVs (wAUV) emulated erythrocytal membranes^[27] (Supplementary

Information). In all these cases only additive changes in the negative bands for AUV samples were observed, suggesting marginal contributions from membrane binding (Fig S2). To delineate the folding propensities of the mixtures from these and aromatic contributions, CD spectra were recorded in 50% (aq) 2,2,2-trifluoroethanol (TFE) (see also Note in Supplementary Information). The spectra were helical for both libraries, with the minimum retained at 226 nm, which appeared red-shifted from a helical band at 222 nm. This band was stronger in intensity when compared to another helical band at 208 nm (Fig S2).^[24] The effect is notable for aromatic residues locked in *i*, *i*+4 helical spacings.^[21, 23, 28] To explore this, CD spectra in 50% TFE were obtained for a sequence-defined (FK)₁₀ peptide. In this control peptide F alternates with K thereby arranging multiple and overlapping *i*, *i*+4 spacings, which may result in enhanced intensities at 226 nm and further dampening of signal at 208 nm.^[24] Indeed, this was observed (Fig S2). CD spectra for this peptide were more profoundly distorted towards the minimum at 226 nm (Fig S2). Taken together, the findings confirm that each mixture contains peptides that are prone to adopt helix-like conformations. The data also indicates that Fk mixtures comprise peptides forming stabilised phenylalanyl stretches, with left-handed D-lysyl breaking homochirality in folding.

Such structures may oligomerize via patterns that are altogether different from those of homochiral peptides. Given that folding did not change in membranes, we sought for a direct evidence of peptide assembly in phospholipid bilayers. Similar to AMPs,^[29] both mixtures should have sufficient freedom for lateral diffusion. However, only contiguous 20-mer homochiral helices, which span 3 nm and match the bilayer thickness of 3.2 nm,^[30] can progressively recruit into transmembrane pores.^[31]

To test this conjecture, we performed nanoscale topographic (atomic force microscopy – AFM) and chemical (secondary ion mass-spectrometry – SIMS) imaging on supported lipid bilayers (SLBs) prepared by AUV deposition on appropriate substrates.^[31] These SLB preparations provide ideal experimental models for fluid-state membranes, access nano-to-micrometre length scales and allow accurate topographic (height) measurements by AFM in relation to the flat surface of SLBs (to within ~0.1 nm).^[32] The same SLBs can be imaged by SIMS which permits detailed visualisation of compositional chemistry with lateral resolution of <100 nm.^[33]

Because AMPs lyse bacteria rapidly and within the doubling time of bacterial cells (20-30 min),^[1-3, 6] the impact of each mixture on SLBs was expected within the same timescale.^[26, 31] SLB samples were separately incubated for 30 min with FK and Fk mixtures that were ¹⁵N-labeled at all phenylalanyl residues. After excess peptide was removed by washing, the hydrated samples were rapidly frozen, freeze-dried and imaged. The same samples were used for AFM and SIMS imaging. Such correlative imaging revealed heterogeneous pore-like structures with a mean diameter of 212.6 ± 92.8 nm for the samples treated with the FK mixtures (Figs 2A, B, Figs S3 & S4). The pores appeared to be filled with particulate aggregates as opposed to interior-free perforations, more common for AMPs. Similar aggregates were apparent across the whole scanned area and tended to assemble into pore-connecting ridges suggesting dynamic peptide migration.^[31] SIMS analyses unambiguously confirmed that the

observed features were peptide-specific. The hue saturation images (HSI) showed $^{12}\text{C}^{15}\text{N}/^{12}\text{C}^{14}\text{N}$ ratios that were far above natural abundance values of 0.37% for the pores, and in the larger pores, where the peptide content was the highest, was nearly 100% (Fig 2B, S4). In contrast, no pore-like structures were observed for the samples incubated with the Fk mixtures (Fig 2A, B). These differences are striking in two regards.

First of all, this is the first visual evidence of stereochemically comparative poration employing model membranes. Secondly, filled pores have not been observed before, while poration mechanisms using random-sequence mixtures had yet to be demonstrated. Hence, this finding prompts a distinctive poration scenario of different homochiral sequences inducing different poration modes. Since pore formation requires cooperative peptide assembly these modes are not necessarily competing, but simultaneous. The measured heights across individual pores, including ridges and interior aggregates, were conservatively 3–4 nm, which agrees with the upward position of peptide helices in the bilayer maximising their contact with hydrophobic lipid tails (Fig 2C & S5).^[26,31] Because all sequences in FK have the same chirality they fold as rod-like, contiguous helices that incorporate into the bilayer in a similar and cooperative manner. The constituent particulate aggregates are intriguing and may derive from inter-peptide zipper-like oligomerisation via phenylalanyl residues.^[34] Such side-chain zipping cannot be cooperative for Fk sequences since heterochiral helices lack persistence.

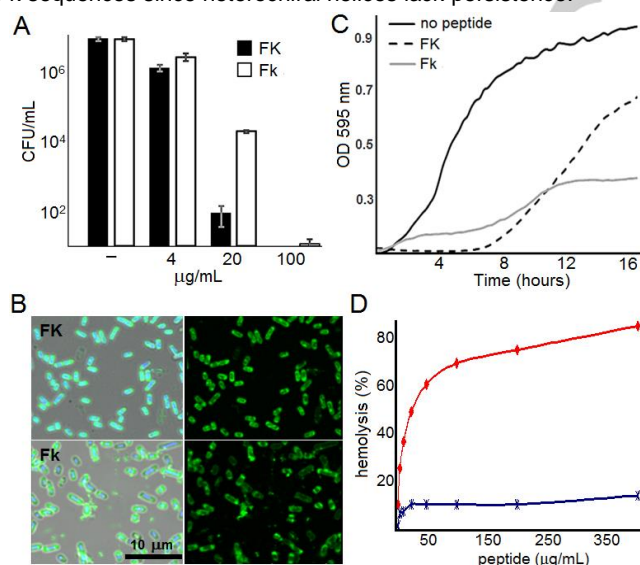


Figure 3. Biological responses. (A) Viability of *E. coli* cells following 10-min incubations with each of the two mixtures at different peptide concentrations. (B) Confocal fluorescence imaging of *E. coli* cells taken after 45-min incubations with carboxyfluorescein-labelled FK and Fk mixtures (50 μg/mL), showing combined (left) and carboxyfluorescein (right) images. The combined images merge phase contrast images and the fluorescence images of peptides (green) and intracellular nucleic acids (blue) stained with 4',6-diamidino-2'-phenylindole (DAPI). (C) OD measurements of *E. coli* in the presence of the mixtures (100 μg/mL) as a function of time. Individual measurements are taken every 15 min. (D) Percentage of hemolysis as a function of peptide concentrations for the homochiral FK (red) and heterochiral Fk (blue) mixtures.

Consequently, a more profound membrane disruption for homochiral pores may manifest in faster killing kinetics.

Consistent with this, minimum inhibitory concentrations (MICs) for the mixtures performed using microdilution assays differed only by one serial dilution, and are therefore comparable (Table S1). In spite of this, antimicrobial responses of the Fk mixtures were weaker in the first 10 minutes in a range of concentrations (Fig 3A).

This is directly relevant to the biology of AMPs, which act within their proteolytic life time, also minutes. With the two mixtures being equally effective in binding to bacterial cells under the first hour of incubation (Fig 3B & S6), only FK peptides kept bacterial growth at negligible rates over the first several hours (up to 11–12 hours in Fig 3C). Longer incubations (>12 hours) were subject to inoculum effects that were similar for the mixtures suggesting peptide depletion during the process (Fig 3C).^[35] The findings indicate that the homochiral sequences are stronger or faster membrane-disrupters, but are equally subject to inoculum-related depletion typical of antibiotics.^[35,36] Implicitly the differences explain profound hemolytic activities observed for the homochiral mixtures (Table S1 & Fig 3D). The mixtures lysed human erythrocytes within the timescale of their antimicrobial action (under an hour) at concentrations as low as 25 μg/mL (Fig 3B, D). In comparison, no progressive lysis (≤10%) was observed for Fk peptides even at concentrations close to the millimolar range (Fig 3D), indicating that helical folding is not a pre-requisite for antimicrobial activity.^[15–17] The FK mixtures are not devoid of hydrophobic helices, which could resemble cytotoxic venom or neurotoxin peptides (e.g. melittin, pardaxin). These toxins target zwitterionic lipids that are exclusive in mammalian cells and predominate in microbial cells. The activity of these peptides relies on exceeding a threshold peptide density on membrane surfaces rather than on apparent poration. As a result, the peptides accumulate into carpet-like structures that disrupt membrane fluidity and cause bilayer rupture.^[37] The Fk mixtures may also contain hydrophobic sequences. However, chirality in diastereomeric sequences is disrupted, disfavoring contiguous and potentially hemolytic conformations. Although erythrocytic lipids are also zwitterionic, red blood cells carry a weak negative charge, which may encourage poration. Complementary to this, both mixtures produced CD signals that appeared stronger in AUVs and wAUVs than in ZUVs (Fig S2). Nevertheless, AFM revealed that SLBs prepared from wAUVs and treated with the mixtures were featureless (Fig S6).

The role of antimicrobial poration is established for homochiral peptides without cross-comparison with heterochiral sequences. Different homochiral compositions can encode poration mechanisms that enable stronger and faster antimicrobial responses.^[3,10,26,31] In such designs, amphipathicity defines the extent of polar and hydrophobic faces precisely, ensures a better control over selectivity and is crucial for pore formation. Hemolysis, on the other hand, does not depend on poration. Even pores induced by bacterial cytolysins are meant for nutrient supply rather than direct cell destruction. Osmotic phenomena, cell depolarization and membrane thinning better explain hemolytic mechanisms, which are readily caused by hydrophobic structures that displace lipids without assembling into higher oligomers or pores. This is in accord with the hemolytic activities of predominantly hydrophobic antibiotics, alamethicin and

gramicidins. Their sequences incorporate non-proteinogenic amino-acids or alternate L- and D-epimers to fold into α (alamethicin) or β (gramicidins) helices,^[38] which provide specialist cases for the formation of small ion channels. Strictly speaking, heterochiral sequences do not appear to cause membrane disruption and may favour intracellular modes of action. However, the formation of small channels by the Fk peptides could not be entirely excluded. Indeed, nearly identical MIC values for both mixtures, with the faster antimicrobial responses for FK peptides, indicate similar mechanisms of action with different degrees of membrane disruption or permeability. In summary, we have demonstrated a mechanistic rationale of relating peptide stereochemistry to differential cytolytic activities. To avoid any sequence-defined bias, all sequences were made random in composition, but of controllable chain length. Each library was assembled from the same two amino acids, only one of which had the same chirality. We showed that, irrespective of peptide chirality, the equimolar ratio of the two amino-acid types used is sufficient for strong antimicrobial activities against Gram positive and Gram negative bacteria, including “superbugs” MRSA and VRE. We further showed that persistence in chirality – homochiral sequences – defines non-differential cytolytic effects, which are accompanied by cooperative pore formation in anionic microbial-like membranes. Only homochiral sequences can fold as contiguous helices, which proved to be necessary for antimicrobial poration, but not for biological activity. Indeed, heterochiral sequences that lack such persistence selectively attack bacterial membranes without poration. All in all, the results hold promise for designing membrane-selective antimicrobials based on relatively short and sequence-random peptides.

Acknowledgements

We thank Sam Gellman for his advice and support of this work. We acknowledge funding from the Israel Ministry of Health for research projects and fellowship fund on food and nutrition with implications on public health (Grant number: 3-11626) and from the European Metrology Research Programme (EMRP) projects. The EMRP is jointly funded by the EMRP participating countries within EURAMET and the European Union.

Keywords: antibiotics • MRSA • nanoscale imaging • protein design • diastereomers

- [1] Czaplewski, L. et al. *Lancet Infect Dis*, **2016**, 16, 239.
- [2] Haney, E. F., Mansour, S. C. & Hancock, R. E. *Methods Mol Biol*, **2017**, 1548, 3.
- [3] Fjell, C. D., Hiss, J. A., Hancock, R. E. & Schneider, G. *Nat. Rev. Drug Discov*, **2012**, 11, 37.

- [4] da Cunha, N. B. et al. *Drug Discov Today*, **2017**, 22, 234.
- [5] McArthur, A. G. et al. *Antimicrob Agents Chemother*, **2013**, 57, 3348.
- [6] Ryan, L. et al. *J Biol Chem*, **2013**, 288, 20162.
- [7] Ishikawa, K., Medina, S. H., Schneider, J. P. & Klar, A. J. *Cell Chem. Biol.*, **2017**, 24, 149.
- [8] Pouny, Y., Rapaport, D., Mor, A., Nicolas, P. & Shai, Y. *Biochemistry*, **1992**, 31, 12416.
- [9] Andreu, D., Merrifield, R. B., Steiner, H. & Boman, H. G. *Biochemistry*, **1985**, 24, 1683.
- [10] Peschel, A. & Sahl, H. G. *Nat. Rev. Microbiol.*, **2006**, 4, 529.
- [11] Cheng, R. P., Gellman, S. H. & DeGrado, W. F. *Chem. Rev.*, **2001**, 101, 3219.
- [12] Porter, E. A., Wang, X., Lee, H. S., Weisblum, B. & Gellman, S. H. *Nature*, **2000**, 404, 565.
- [13] Shai, Y. *Biopolymers*, **2002**, 66, 236.
- [14] Yang, L., Harroun, T. A., Weiss, T. M., Ding, L. & Huang, H. W. *Biophys J*, **2001**, 81, 1475.
- [15] Oren, Z., Hong, J. & Shai, Y. *J Biol. Chem.*, **1997**, 272, 14643.
- [16] Huang, Y., He, L., Li, G., Zhai, N., Jiang, H. & Chen, Y. *Protein Cell*, **2014**, 5, 631.
- [17] Shai, Y. & Oren, Z. *Peptides*, **2001**, 22, 1629.
- [18] Hayouka, Z., Chakraborty, S., Liu, R., Boersma, M. D., Weisblum, B. & Gellman, S. H. *J Am Chem. Soc.*, **2013**, 135, 11748.
- [19] Wen, K. E. & Orgel, L. E. *Orig. Life Evol. Biosph.*, **2001**, 31, 241.
- [20] Sreerama, N., Manning, M. C., Powers, M. E., Zhang, J.-X., Goldenberg, D. P. & Woody, R. W. *Biochemistry*, **1999**, 38, 10814.
- [21] Chakraborty, A., Kortemme, T., Padmanabhan, S. & Baldwin, R. L. *Biochemistry*, **1993**, 32, 5560.
- [22] Castelletto, V. & Hamley, I. W. *Biophys Chem.*, **2009**, 141, 169.
- [23] Shibata, A., Murata, S., Ueno, S., Liu, S., Futaki, S. & Baba, Y. *Biochim. Biophys. Acta*, **2003**, 1616, 147.
- [24] Ryadnov, M. G. & Woolfson, D. N. *J Am Chem. Soc.*, **2005**, 127, 12407.
- [25] Lin, W. C., Blanchette, C. D. & Longo, M. L. *Biophys J*, **2007**, 92, 2831.
- [26] Pyne, A. et al. *Chem. Sci.*, **2017**, 8, 1105.
- [27] Himbert, S. et al. *Sci Rep.*, **2017**, 7, 39661.
- [28] Guyader, C. P., Lamarre, B., De Santis, E., Noble, J. E., Slater, N. K. & Ryadnov, M. G. *Sci Rep.*, **2016**, 6, 35012.
- [29] Yu, Y., Vroman, J. A., Bae, S. C. & Granick, S. *J Am Chem. Soc.*, **2010**, 132, 195.
- [30] Kucerka, N., Nieh, M. P. & Katsaras, J., *Biochim Biophys Acta*, **2011**, 1808, 2761.
- [31] Rakowska, P. D. et al. *Proc. Natl. Acad. Sci. USA*, **2013**, 110, 8918.
- [32] Lin, W. C., Blanchette, C. D., Ratto, T. V. & Longo, M. L. *Methods Mol. Biol.*, **2007**, 400, 503.
- [33] Kraft, M. L., Weber, P. K., Longo, M. L., Hutcheon, I. D. & Boxer, S. G. *Science*, **2006**, 313, 1948.
- [34] Hayouka, Z., Mortenson, D. E., Kreidler, D. F., Weisblum, B., Forest, K. T. & Gellman, S. H. *J Am Chem. Soc.*, **2013**, 135, 15738.
- [35] Jepson, A. K., Schwarz-Linek, J., Ryan, L., Ryadnov, M. G. & Poon, W. C. *Adv Exp Med Biol.*, **2016**, 915, 33.
- [36] Brook, I. *Rev Infect Dis.*, **1989**, 11, 361.
- [37] Hallock, K., Lee, D., Omnass, J., Mosberg, H. & Ramamoorthy, A. *Biophys J*, **2002**, 83, 1004.
- [38] Gurnev, P. A. & Nestorovich, E. M. *Toxins (Basel)*, **2014**, 6, 2483.

COMMUNICATION

Entry for the Table of Contents (Please choose one layout)

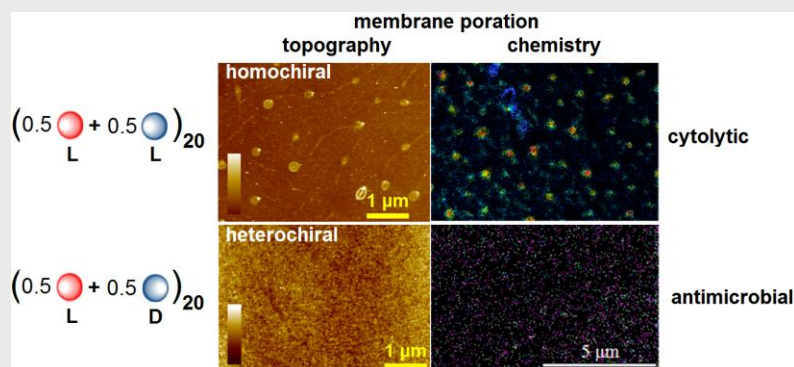
Layout 2:

COMMUNICATION

Zvi Hayouka,* Angelo Bella, Tal Stern,
Santanu Ray, Haibo Jiang, Chris R. M.
Grovenor and Maxim G. Ryadnov*

Page No. – Page No.

Binary encoding of peptide
sequences into differential
antimicrobial mechanisms



Random sequences assembled from two amino acids with varied chirality selectively lyse bacteria including "superbugs" MRSA and VRE.